Effects of Reduced Sulfur Compounds on Pd-catalytic Hydrodechlorination of TCE in Groundwater by Cathodic H$_2$ under Electrochemically-induced Oxidizing Conditions

Songhu Yuan[*,†,‡], **Mingjie Chen**[§], **Xuhui Mao**[‡], and **Akram N. Alshawabkeh**[*,‡]

[†]State Key Lab of Biogeology and Environmental Geology, China University of Geosciences, 388 Lumo Road, Wuhan, 430074, P. R. China

[‡]Department of Civil and Environmental Engineering, Northeastern University, 400 Snell Engineering, 360 Huntington Avenue, Boston, Massachusetts 02115, United States

[§]Atmospheric, Earth and Energy Division, Lawrence Livermore National Laboratory, P.O. Box 808, L8184, Livermore, CA 94550, United States

Abstract

Reduced sulfur compounds (RSCs) poison Pd catalysts for catalytic hydrodechlorination of contaminants in anoxic groundwater. This study investigates the effects of RSCs on Pd-catalytic hydrodechlorination of trichloroethylene (TCE) in oxic groundwater. Water electrolysis in an undivided electrolytic cell is used to produce H$_2$ for TCE hydrodechlorination under oxidizing conditions. TCE is efficiently hydrodechlorinated to ethane, with significant accumulation of H$_2$O$_2$ under acidic conditions. Presence of sulfide at concentrations less than 93.8 μM moderately inhibits TCE hydrodechlorination and H$_2$O$_2$ production. Presence of sulfite at low concentrations (1 mM) significantly enhances TCE decay, while at high concentration (3 mM) inhibits initially and enhances afterwards when sulfite concentration declines to less than 1 mM. Using radical scavenging experiments and electron spin resonance assay, SO$_3^{\bullet-}$ which is generated from sulfite under oxidizing conditions is validated as the new reactive species contributing to the enhancement. This study reveals a distinct mechanism of effect of sulfite on TCE hydrodechlorination by Pd and H$_2$ in oxic groundwater and presents an alternative approach to increasing resistance of Pd to RSCs poisoning.

INTRODUCTION

Contamination of groundwater by chlorinated hydrocarbon compounds (CHCs), such as trichloroethylene (TCE) and perchloroethylene (PCE), continues to be a serious world-wide environmental problem.[1] Pd-catalytic hydrodechlorination is a process that is proposed and tested for transformation of CHC contamination. A variety of CHCs can be rapidly hydrodechlorinated to less toxic or nontoxic and more readily biodegradable substances.[2–8] Field applications prove that the performance of Pd-catalytic hydrodechlorination of CHCs by H$_2$ can be sustained for several years.[9–11] Typically H$_2$ is supplied as a compressed gas. Groundwater is saturated with H$_2$, and then passes through a Pd catalyst bed, wherein CHCs are hydrodechlorinated. However, there are a few barriers for full-scale implementation. Transportation and storage of compressed H$_2$ gas is dangerous and injecting H$_2$ into

subsurface is relatively costly. Furthermore, the catalytic activity of Pd significantly decreases in the presence of reduced sulfur compounds (RSCs), such as sulfite and sulfide, generated from sulfate-reducing bacteria respiration in anoxic aquifers.[5,9,11] Oxidizing reagents, such as hypochlorite,[5,9,12] hydrogen peroxide,[10] and permanganate,[13] can regenerate sulfur-fouled Pd catalyst to some extent. However, the periodic flushing of catalyst bed with oxidizing reagent complicates the operation when applied in situ. Therefore, it is crucial to seek new strategies to supply H_2 safely and expediently and to increase the resistance of Pd to RSCs fouling.

Water electrolysis at a cathode (eq. 1) provides an alternative approach for supplying H_2 in situ. A preliminary investigation shows that TCE in groundwater could be hydrodechlorinated using H_2 produced by an undivided electrolyzer.[14] Our recent work also proves the feasibility of in situ supplying of cathodic H_2 for 2,4-dichlorophenol hydrodechlorination in a divided electrolytic cell.[15] In both investigations, the electrolytic system was the sole source of H_2, and the other products, i.e., O_2, from water electrolysis (eq. 2) were assumed to inhibit hydrodechlorination.[14,15] Nevertheless, production of O_2 at the anode is inevitable when water electrolysis happens. Significant accumulation of H_2O_2 (> 20 mg/L) occurs in an undivided electrolytic cell in the presence of Pd catalyst under acidic conditions (eq. 3) in addition to H_2O (eq. 4), and low concentrations of strongly oxidizing •OH radicals (oxidation potential: 2.8 V vs standard hydrogen electrode, SHE) were also measured (eq. 5).[16,17] Reactive oxygen species (ROSs), i.e., H_2O_2, •OH and dissolved O_2, can oxidize RSCs in aqueous solution.[18–21] The efficient oxidation of sulfide in wastewater at mixed metal oxide coated titanium (Ti/MMO) electrode was recently reported.[22,23] As a result, when water electrolysis at inert electrodes, i.e., Ti/MMO, is used to supply H_2 for Pd-catalytic hydrodechlorination of CHCs in groundwater, Ti/MMO electrode and the simultaneously generated ROSs can potentially oxidize RSCs, thereby increasing the resistance of Pd to the fouling by RSCs. However, the activity of Pd catalysts when impacted by the presence of RSCs under oxidizing conditions is still not clear.

$$2H_2O + 2e^- \rightarrow H_2 + 2OH^- \quad (1)$$

$$2H_2O \rightarrow O_2 + 4H^+ + 4e^- \quad (2)$$

$$H_2 + O_2 \xrightarrow{Pd} H_2O_2 \quad (3)$$

$$2H_2 + O_2 \xrightarrow{Pd} 2H_2O \quad (4)$$

$$H_2O_2 \xrightarrow{Pd} 2 \bullet OH \quad (5)$$

In this study, water electrolysis in undivided electrolytic cells is used to produce H_2 and oxidizing conditions. The effects of RSCs, sulfide (sulfide and bisulfide) and sulfite (sulfite and bisulfite), on H_2O_2 generation and Pd-catalytic hydrodechlorination of TCE in simulated groundwater are investigated in a batch mode. The process can be also simulated in a flow-through mode although it is not conducted.[24] As reactions differ greatly under oxidizing and reducing conditions, special attention is paid to the mechanisms of influence of RSCs.

EXPERIMENTAL SECTION

Chemicals

TCE (99.5%) and cis-dichloroethylene (cis-DCE, 97%) were purchased from Sigma-Aldrich. H_2O_2 (30%) and Na_2SO_3 (98.1%) were purchased from Fisher Sci. $Na_2S \cdot 9H_2O$ (98%) and L-ascorbic acid sodium salt (99%) were obtained from Acros. 5,5-dimethyl-1-pyrroline-N-oxide (DMPO) was provided by Cayman Chemical Company (USA). Gas standard (1% (v/v) methane, ethene, ethane, acetylene, CO_2 and CO in nitrogen) was supplied by Supelco. Excess TCE was dissolved into 18.2 MΩ·cm high-purity water to form a TCE saturated solution (1.07 mg/mL at 20 °C), which was used as stock solution for preparing aqueous TCE solutions. Palladium on alumina powder (1% wt. Pd, Sigma-Aldrich) with average particle size of 6 Qm was used as catalyst in batch experiments. Deionized water (18.0 MOPcm) obtained from a Millipore Milli-Q system was used in all the experiments. All chemicals used in this study were above analytical grade.

TCE Hydrodechlorination in an Undivided Electrolytic Cell

The same experimental setup as reported previously[17] is used for TCE hydrodechlorination at ambient temperature. As shown in Figure S1, a 150-mL syringe with a plunge was connected to the cell, allowing gas expansion during electrolysis. Two pieces of Ti/MMO (coated with IrO_2/Ta_2O_5, mesh type, 3N International, USA) with dimensions of 85 mm length by 15 mm width and 1.8 mm thickness were used as anode and cathode with 42 mm spacing in parallel position. For each test, 400 mL of 10 mM Na_2SO_4 solution was transferred into the cell, and 1 g/L Pd/Al_2O_3 were attained by addition of specific mass of Pd/Al_2O_3 powder. Na_2SO_3 powder and Na_2S stock solution (6 mM) were added, respectively. 10 mL of TCE saturated water was then added to produce an initial concentration of 198 μM (26.1 mg/L). The reactor was sealed immediately and the solution was stirred (600 rpm) for 10 min to allow equilibrium of TCE in the aqueous solution. A constant electric current of 100 mA ($10 mA/cm^2$) was applied with a cell voltage of about 7 V. The aqueous solution was sampled for analysis of TCE, *cis*-DCE, pH and H_2O_2 concentrations. Gas samples were collected from specific experiments for headspace gas analysis.

Chemical Analysis

TCE and cis-DCE concentrations were measured by a 1200 Infinity Series HPLC (Agilent) equipped with a 1260 diode array detector and a Thermo ODS Hypersil C18 column (4.6×50 mm). The mobile phase was a mixture of acetonitrile and water (60:40, v/v) at 1 mL/min. The detection wavelength was 210 nm. Ethene and ethane in the headspace were detected by Model 310 GC (SRI, USA) with flame ionization detector and Haysep-T column. 100 μL of headspace gas was sampled and injected from an on-column port. The temperature program includes heating the column from 40 to 140 °C at a rate of 15 °C/min, holding the temperature at 140 °C for 1 min, and then cooling to 40 °C at a rate of 20 °C/min. For the batch experiments, gas concentrations of TCE and aqueous concentrations of ethane were calculated by Henry's law, and the sum of aqueous and gas concentrations was derived.

Sulfite at concentrations higher than 1 mM was also measured by HPLC using the same procedure as for TCE analysis. Sulfide was detected at 665 nm on a spectrometer (Spectronic 20D+, Caley & Whitmore Corp.) after coloration with dimethyl-p-phenylene,[25] and H_2O_2 was analyzed at 405 nm after coloration with $TiSO_4$.[26] Generation of new radicals in the presence of sulfite was assayed by electron spin resonance (ESR). 100 μL sample collected from the batch system without contaminants was immediately mixed with 25 μL of 0.2 M DMPO to form DMPO-radical adduct, which was then measured within 10 min on a Bruker EMX ESR spectrum with microwave bridge (receiver gain, 5020; modulation

amplitude, 2 Gauss; microwave power, 6.35 mW; modulation frequency, 100 kHz; center field: 348.5 mT).

Data Analysis

Langmuir-Hinshelwood (L–H) model is generally employed to describe the kinetics of heterogeneous hydrodechlorination on Pd surface assuming the reaction is controlled by surface reaction.[27–29] As the production of H_2 is identical at the same current and the adsorption of H_2 on Pd surface is strong,[27,28] the concentration of adsorbed H on Pd surface can be assumed to be constant. Therefore, L–H model is expressed as

$$-\frac{dc}{dt} = kS = k\frac{K_A c}{1 + K_A c} \quad (6)$$

where c is the aqueous concentration of TCE (μM), t is the reaction time (min), k is the surface reaction rate constant (min^{-1}), S is TCE coverage on Pd surface (μM), and K_A is Langmuir adsorption coefficient of TCE on reactive sites (μM^{-1}). MATLAB (Version 2010b) was used for data calculation.

RESULTS AND DISCUSSION

Pd-Catalytic TCE Hydrodechlorination and H_2O_2 Accumulation in the Electrolytic System

Control experiments in the absence of Pd/Al$_2$O$_3$ show limited removal of TCE (Figure S2), which was ascribed to the direct reduction on the Ti/MMO cathode[30] and the possibility of limited oxidation of TCE on the Ti/MMO anode. In the presence of 1 g/L Pd/Al$_2$O$_3$, TCE was efficiently reduced in the undivided electrolytic cell in a wide pH range with accumulation of ethane (Figure 1a), confirming that Pd-catalytic hydrodechlorination was the dominant pathway for TCE transformation even in the presence of anodic O$_2$. This agrees well with previous results.[14,17] The mass balance of TCE and ethane is about 80%, implying the presence of other intermediates that were not quantified.[6,31] Quantification of all the intermediates was not performed as the sum of TCE and ethane can support the dominant pathway. The contribution of bipolar electrodes of Pd/Al$_2$O$_3$ particles induced by electric field (7 V) to TCE transformation is negligible due to the small particles size (6 Qm) and low particle concentration (1 g/L).[32]

Fitting TCE decay by eq. 6 shows that K_A values are in the level of 10^{-5} μM^{-1}, which is consistent with the negligible adsorption of TCE on Pd catalyst.[17] As $K_A c$ is much less than 1, L–H model approaches pseudo-first-order kinetics (eq. 7)

$$-\frac{dc}{dt} = kK_A c = k_{obs} c \quad (7)$$

where k_{obs} (= kK_A) is the observed pseudo-first-order rate constant. Table 1 shows that the hydrodechlorination is well represented by pseudo-first-order kinetic model ($R^2 > 0.950$), supporting the above approximation of L-H model. In the wide pH range from 10.5 to 3.0, the observed rate constant (k_{obs}) only changed when pH dropped from 5.5 (0.010 min^{-1}) to 4.0 (0.014 min^{-1}). Pd-catalytic hydrodechlorination of TCE generally increases with increasing solution pH under anoxic conditions due to neutralization of acids produced,[2,5,33] so the different influence of pH observed in this study can be ascribed to the presence of O$_2$. The rate constant of TCE transformation normalized by Pd concentration (0.01 g$_{Pd}$/L) is about 1 L g$_{Pd}^{-1}$ min^{-1}, which is in the comparable level as those reported using Pd and H$_2$ for TCE hydrodechlorination.[2,5,33]

A comparison of TCE hydrodechlorination in the cathodic compartment shows that anodic O_2 greatly suppressed TCE hydrodechlroiantion (Figure S3). The observed rate constant at 50 mA increased to 0.071 min^{-1}, which is about 5 times that in the presence of anodic O_2 at 100 mA (Experiments. 2 and 7 in Table 1). In comparison, the decay of TCE is negligible in the anodic compartment (Figure S4). The remarkable inhibition of O_2 on TCE hydrodechlorination was due to competition of O_2 for the active H and the block of TCE reaction with H by the chemisorbed O_2 on Pd surface.[34] Similar inhibitory effect of O_2 is also revealed in Pd-catalytic hydrodechlorination studies.[6,14,34] Because O_2 is proportionally generated with the production of H_2 in an undivided electrolytic cell, its inhibition is inevitable. However, this mode of H_2 supply can be easily applied in situ and may potentially control Pd poisoning by RSCs in groundwater.

In the undivided electrolytic system, O_2 produced at the anode competed with TCE for Pd•[H].[6,14] Aside from the production of H_2O, the combination of chemisorbed H_2 and O_2 on Pd surface can produce H_2O_2 (eq. 5).[16,17,35,36] H_2O_2 can also be produced through O_2 reduction on the MMO cathode, but this contribution is of minor importance in the presence of Pd catalyst.[17,24] Figure 1b shows that H_2O_2 accumulation increased with decreasing solution pH. However, TCE hydrodechlorination only slightly increased with decreasing solution pH from 5.5 to 4 (Figure 1a). This suggests that H_2O_2 accumulation did not significantly inhibit TCE hydrodechlorination. The oxidation-reduction potential (ORP) at pH 4 increased up to 375 mV within 80 min.[17] As a result, it is feasible to supply H_2 for Pd-catalytic hydrodechlorination under electrochemically generated oxidizing conditions. Moreover, the generated H_2O_2 provides a potential oxidant to increase the resistance of Pd to RSCs fouling.[18–20]

Effect of Sulfide

With the increase in sulfide concentration from 0 to 93.8 μM, TCE hydrochlorination was increasingly inhibited (Figures 2a) and the rate constant decreased from 0.0.014 to 0.006 min^{-1} (Table 1). H_2O_2 production was negligibly affected at sulfide concentration less than 31.3 μM, but was significantly inhibited at 93.8 μM sulfide (Figure S5a). This suggests that the influence of sulfide on the reaction of active H with O_2 is less as pronounced as with TCE. The inhibition can be attributed to the poisoning of Pd catalyst by sulfide, i.e., formation of Pd–S complex.[12] The trend of sulfide influence on TCE hydrodechlorination agrees with those reported under anoxic conditions,[2,5,12,37,38] but the inhibition is less significant compared with the literature.[5] The oxidation of sulfide using MMO electrode was reported[22–23] and was also observed in this study (Figure S6). During the course of hydrodechlorination, sulfide was not detected in solution. Control experiments without electrolysis prove that sulfide was completely adsorbed by Pd/Al$_2$O$_3$ particles within 2 min. Since sulfide can be oxidized by H_2O_2 and ROSs,[20–23] it is rationale to infer that sulfide can be oxidized by the as-formed H_2O_2 and •OH on Pd surface. Consequently, the resistance of Pd catalyst to sulfide poisoning increased under the electrochemically-induced oxidizing conditions.

Distinct Effect of Sulfite

Unexpectedly, sulfite shows a unique influence on TCE hydrodechlorination. When sulfite concentration increased from 0 to 1 mM, TCE transformation remarkably increased (Figure 2b) with the increase in k_{obs} from 0.014 to 0.022 min^{-1} (Table 1). The total carbon decreased in the initial 40 min and increased afterwards (Figure S7), which indicates the production of undetected intermediates. The predominant production of ethane proves that hydrodechloriantion is still the dominant transformation pathway. The presence of sulfite at concentrations less than 1 mM has slight influence on H_2O_2 accumulation (Figure S5b). In the presence of 3 mM sulfite, TCE transformation in the initial 60 min was lower than that

without sulfite and negligible H_2O_2 was accumulated, whereas both TCE transformation and H_2O_2 accumulation promptly increased after 60 min. Measurements show that 3 mM sulfite was oxidized to less than 1 mM at 60 min in the system (Figure S8). This is consistent with the observation that TCE decay was enhanced in the presence of less than 1 mM sulfite. The slower transformation of TCE during the initial 60 min was due to Pd poisoning caused by the high concentration of sulfite.[37,38]

Identification of Reactive Species due to the Unique Influence of Sulfite

Enhancement of Pd-catalytic hydrodechlorination by the presence of low concentrations of sulfite has never been reported before. In contrast, inhibition of Pd activity towards TCE hydrodechloriantion by sulfite has been well recognized under anoxic conditions.[2,5,12,13,37,38] Therefore, the enhancement at low sulfite concentrations is attributed to the presence of O_2 and ROSs, i.e., the production of new reactive species from sulfite or the alleviation of O_2 inhibition through scavenging dissolving O_2. A series of comparison experiments were therefore conducted to elucidate the mechanism. (1) TCE transformation at the electrode in the absence of Pd was minute, and was even slightly suppressed by the presence of 1 mM sulfite (Figure S9). This suggests that electrode reactions can not lead to the enhancement. (2) At a high pH of 10.5 in the presence of Pd without H_2O_2 accumulation, the presence of 1 mM sulfite led to marginal influence (Figure S10). So, the alleviation of O_2 inhibition was not responsible for the enhancement, and the in situ generated H_2O_2 probably contributed. It is noted that the trends of H_2O_2 accumulation at different concentrations of sulfite (Figure S5b) were similar to those of TCE decay (Figure 2b), which further supports the possible contribution of H_2O_2. (3) Without electrolysis in the absence of Pd, TCE degradation by H_2O_2 and 1 mM sulfite was negligible (Figure 3a), ruling out the contribution of free H_2O_2 to the production of new reactive species from sulfite. (4) Without electrolysis and in the presence of Pd, the transformation by H_2O_2 was also minimal but became significant after addition of 1 mM sulfite (Figure 3a). As a consequence, the combination of H_2O_2 and Pd, that is, the chemisorbed H_2O_2 on Pd surface and the •OH generated from the decomposition of chemisorbed H_2O_2,[16,17] is responsible for the enhancement.

The oxidation of sulfite by H_2O_2 and •OH has been extensively investigated.[18,39,40] Sulfite can be oxidized to $SO_3^{•-}$ by activated H_2O_2[39,40] and •OH (eq. 8),[41] which was validated by ESR assay in our recent study.[24] $SO_3^{•-}$ combines with O_2 forming $SO_5^{•-}$ quickly (eq. 9), which may transform to HSO_5^- under acidic conditions (eq. 10) and further to $SO_4^{•-}$ at a slow rate (eq. 11). Therefore, the chemisorbed H_2O_2 and •OH in this study were able to initiate these radical chain reactions, and the oxidizing radicals, including •OH (2.8 V/SHE), $SO_4^{•-}$ (2.5–3.1 V/SHE[42]), HSO_5^- (1.82 V/SHE[41]), $SO_5^{•-}$ (1.1 V/SHE[41]) and $SO_3^{•-}$ (0.6 V/SHE[41]), may contribute to TCE decay.

$$HSO_3^- + \bullet OH \rightarrow SO_3^{•-} + H_2O \qquad k_2 = 9.5 \times 10^9 \quad M^{-1} \quad s^{-1}\,{}^{41} \quad (8)$$

$$SO_3^{•-} + O_2 \rightarrow SO_5^{•-} + OH^- \qquad k_2 = 1.5 \times 10^9 \quad M^{-1} \quad s^{-1}\,{}^{41} \quad (9)$$

$$SO_5^{•-} + H^+ + e^- \rightarrow HSO_5^- \quad (10)$$

$$SO_5^{•-} + HSO_3^- \rightarrow SO_4^{•-} + HSO_4^- \qquad k_2 = 3.0 \times 10^6 \quad M^{-1} \quad s^{-1}\,{}^{41} \quad (11)$$

The contributions of oxidizing radicals were first examined by radical scavenging experiments. Ascorbic acid is a common oxidizing radical scavenger.[43] In the presence of ascorbic acid, TCE decay was inhibited to some extent, approaching that without sulfite (Figure 3b). This proves that the oxidation pathway, which was presumably in parallel to hydrodechlorination pathway, was accountable for the enhanced transformation in the presence of 1 mM sulfite. Methanol can effectively scavenge $\bullet OH$ and $SO_4^{\bullet-}$.[42] Slightly inhibitory effect was observed by the addition of methanol (Figure 3b), suggesting the minute contribution of $\bullet OH$ and $SO_4^{\bullet-}$. The difference of the inhibition caused by ascorbic acid and methanol can be assigned to the contribution of radicals with moderately oxidizing ability, i.e., $SO_3^{\bullet-}$ and $SO_5^{\bullet-}$.

The generation of radicals is then measured by ESR assay. Figure 4a shows that control electrolysis experiments with 1 mM sulfite without Pd as well as with Pd without sulfite demonstrate insignificant radical signals (Curves 1 and 2). This precludes the generation of radicals through the possible reactions of DMPO with anode, sulfite, Pd or H_2O_2.[44] In the presence 1 mM sulfite and Pd, clear radical signals with hyperfine coupling constants of $a^N = 14.9$ G and $a^H = 14.9$ G were observed (Curve 3). The feature is consistent with that of DMPO/$\bullet OH$.[19] However, the contribution of $\bullet OH$ to TCE transformation has been verified to be minimal. It was reported that DMPO/$SO_3^{\bullet-}$ adduct is unstable and transforms to DMPO/$\bullet OH$ within minutes.[45,46] The time profile of the ESR signals for the sample taken from the system with 1 mM sulfite and Pd (Figure 4b) clearly revealed the existence of DMPO/$SO_3^{\bullet-}$ which has the featured hyperfine coupling constants of $a^N = 14.7$ G and $a^H = 16.0$ G.[46,47] It was also observed that the signals of DMPO/$SO_3^{\bullet-}$ decreased quickly within 4 min accompanied with the increase of the signals of DMPO/$\bullet OH$, proving the transformation of DMPO/$SO_3^{\bullet-}$ to DMPO/$\bullet OH$. Therefore, DMPO/$\bullet OH$ observed with Pd and 1 mM sulfite in Figure 4a can be assumed to result from DMPO/$SO_3^{\bullet-}$. When sulfite concentration is elevated to 3 mM, the radical signals became very weak (Curve 4, Figure 4a), due to the scavenging of oxidizing radicals by the high concentrations of sulfite.

As a summary, the enhancement in the presence of low concentrations of sulfite is mostly ascribed to the generation of new ROSs. $SO_3^{\bullet-}$ was confirmed as the new ROS produced from sulfite and chemisorbed H_2O_2 and $\bullet OH$. Because $SO_3^{\bullet-}$ can react with O_2 producing $SO_5^{\bullet-}$ at a diffusion-controlled rate (eq. 9),[41] $SO_5^{\bullet-}$ is assumed to be the secondary ROS. $SO_5^{\bullet-}$ was not measured because of the extremely weak ESR response.[46] The oxidation potentials of $SO_5^{\bullet-}$ and $SO_3^{\bullet-}$ are 1.1 and 0.6 V, respectively.[44] The activation barrier for TCE oxidation decreased to zero at an electrode potential of 1.6 V according to density function calculation.[48] As a consequence, $SO_5^{\bullet-}$ was most likely to account for the enhanced transformation.

Proposed Mechanisms for the Distinct Effects of RSCs under Oxidizing Conditions

The mechanisms of the distinct influence of sulfide and sulfite are summarized in Scheme 1. At the MMO electrodes, water electrolysis produced H_2 and O_2, and both sulfide and sulfite were oxidized to some extent. H_2 was chemisorbed on Pd surface forming reactive H, which was responsible for the efficient hydrodechlorination of TCE to ethane in the absence of RSCs. O_2 competed with TCE for the reactive H, thus inhibiting the hydrodechlorination. Chemisorbed H_2 and O_2 on Pd surface also generated H_2O_2, leading to oxidation of sulfide. Because the adsorption of sulfide on the Pd surface was quick and the oxidation of sulfide was slow, TCE hydrodechlorination by Pd$\bullet$[H] was somewhat inhibited by sulfide-induced Pd poisoning.

At low sulfite concentrations (1 mM), $SO_3^{\bullet-}$ was produced from sulfite oxidation by chemisorbed H_2O_2 or $\bullet OH$, and then quickly transformed to $SO_5^{\bullet-}$. Both $SO_3^{\bullet-}$ and $SO_5^{\bullet-}$, particularly the later, were assumed to enhance TCE transformation producing

intermediates, which were eventually hydrodechlorinated to ethane. So, the intermediates have 2 or more carbons in the structure. No new peaks appeared in HPLC using 210 nm detection wavelength, suggesting the breakage of C=C double bond. GC-MS analysis also did not detect any relevant compounds even when the sample was concentrated up to 100 times. The undetectable intermediates were responsible for the initial decrease of detected total carbon during TCE hydrodechlorination in the presence of 1 mM sulfite, and the further hydrodechlorination of these intermediates to ethane contributed to the increase of total carbon (Figure S7). At a high sulfite concentration (3 mM), both H_2O_2 and radicals were quickly depleted by sulfite, and surplus sulfite poisoned Pd catalyst suppressing TCE decay. When sulfite was oxidized to less than 1 mM by the MMO anode and ROSs, the pathway of sulfur radical oxidation became significant, and Pd poisoning was eliminated or alleviated.

Implications

This study investigates the effects of RSCs on Pd-catalytic hydrodechlorination of TCE using cathodic H_2 under electrochemically-induced oxidizing conditions. It is feasible to hydrodechlorinate TCE in groundwater using cathodic H_2 even with the simultaneous production of O_2 and H_2O_2. O_2 greatly suppresses TCE hydrodechlorination, whereas H_2O_2 slightly influences TCE hydrodechlorination and contributes to RSCs oxidation. Due to the oxidation by H_2O_2 and MMO anode, the resistance of Pd catalysts towards RSCs poisoning increases. In particular, sulfite can be initiated by H_2O_2 and Pd to form new oxidizing radicals, providing extra contribution to TCE decay through oxidation in parallel to Pd-catalytic hydrodechlorination. This unique mechanism of the influence of sulfite was elucidated for the first time, which contributes to the understanding of Pd-catalytic transformation of contaminants in oxic groundwater. Although the reactions were carried out in a batch mode, similar effects are anticipated in a flow-through mode, i.e., using a special three-electrode column system.[24] As a derivative, ROSs and electric field can inhibit microbial activity,[49,50] and acidic conditions may alleviate precipitate formation from Ca^{2+}, Mg^{2+} etc., hence having the potential to resist fouling by biofilms and precipitates.

Supplementary Material

Refer to Web version on PubMed Central for supplementary material.

Acknowledgments

References

1. Moran MJ, Zogorski JS, Squillage PJ. Chlorinated solvents in groundwater of the United States. Environ. Sci. Technol. 2007; 41:74–81. [PubMed: 17265929]

2. Chaplin BP, Reinhard M, Schneider WF, Schueth C, Shapley JR, Strathmann T, Werth CJ. A critical review of Pd-based catalytic treatment of priority contaminants in water. Environ. Sci. Technol. 2012; 46:3655–3670. [PubMed: 22369144]

3. He F, Zhao D. Hydrodechlorination of trichloroethene using stabilized Fe-Pd nanoparticles: Reaction mechanism and effects of stabilizers, catalysts and reaction conditions. Appl. Catal. B Environ. 2008; 84:533–540.

4. Hildebrand H, Mackenzie K, Kopinke FD. Highly active Pd-on-magnetite nanocatalysts for aqueous phase hydrodechlorination reactions. Environ. Sci. Technol. 2009; 43:3254–3259. [PubMed: 19534143]

5. Lowry GV, Reinhard M. Pd-catalyzed TCE dechlorination in groundwater: Solute effects, biological control, and oxidative catalyst regeneration. Environ. Sci. Technol. 2000; 34:3217–3223.

6. Lowry GV, Reinhard M. Pd-catalyzed TCE dechlorination in water: Effects of [H_2](aq) and H_2-utilizing competitive solutes on the TCE dechlorination rate and product distribution. Environ. Sci. Technol. 2001; 35:696–702. [PubMed: 11349280]

7. Nutt MO, Hughes JB, Wong MS. Designing Pd-on-Au bimetallic nanoparticle catalysts for trichloroethene hydrodechlorination. Environ. Sci. Technol. 2005; 39:1346–1353. [PubMed: 15787376]

8. Yuan G, Keane MA. Aqueous-phase hydrodechlorination of 2,4-dichlorophenol over Pd/Al_2O_3: Reaction under controlled pH. Ind. Eng. Chem. Res. 2007; 46:705–715.

9. Davie MG, Cheng H, Hopkins GD, Lebron CA, Reinhard M. Implementing heterogeneous catalytic dechlorination technology for remediating TCE-contaminated groundwater. Environ. Sci. Technol. 2008; 42:8908–8915. [PubMed: 19192817]

10. Schueth C, Kummer NA, Weidenthaler C, Schad H. Field application of a tailored catalyst for hydrodechlorinating chlorinated hydrocarbon contaminants in groundwater. Appl. Catal. B Environ. 2004; 52:197–203.

11. McNab WW Jr. Ruiz R, Reinhard M. In-Situ destruction of chlorinated hydrocarbons in groundwater using catalytic reductive dehalogenation in a reactive well: Testing and operational experiences. Environ. Sci. Technol. 2000; 34:149–153.

12. Chaplin BP, Shapley JR, Werth CJ. Regeneration of sulfur-fouled bimetallic Pd-based catalysts. Environ. Sci. Technol. 2007; 41:5491–5497. [PubMed: 17822122]

13. Angeles-Wedler D, Mackenzie K, Kopinke FD. Permanganate oxidation of sulfur compounds to prevent poisoning of Pd catalysts in water treatment processes. Environ. Sci. Technol. 2008; 42:5734–5739. [PubMed: 18754501]

14. Mcnab JRWW, Ruiz R. Palladium-catalyzed reductive dehalogenation of dissolved chlorinated aliphatics using electrolytically-generated hydrogen. Chemosphere. 1998; 37:925–936.

15. Zheng MM, Bao JG, Liao P, Wang K, Yuan SH, Tong M, Long HY. Electrogeneration of H_2 for Pd-catalytic hydrodechlorination of 2,4-dichlorophenol in groundwater. Chemosphere. 2012; 87:1097–1104. [PubMed: 22377173]

16. Yuan SH, Fan Y, Zhang YC, Tong M, Liao P. Pd-catalytic in situ generation of H_2O_2 from H_2 and O_2 produced by water electrolysis for the efficient electro-Fenton degradation of rhodamine B. Environ. Sci. Technol. 2011; 45:8514–8520.

17. Yuan SH, Mao X, Alshawabkeh AN. Efficient degradation of TCE in groundwater using Pd and electro-generated H_2 and O_2: A shift in pathway from hydrodechlorination to oxidation in the presence of ferrous ions. Environ. Sci. Technol. 2012; 46:3398–3405. [PubMed: 22315993]

18. Hoffmann MR, Edwards JO. Kinetics of the oxidation of sulfite by hydrogen peroxide in acidic solution. J. Phys. Chem. 1975; 79:2096–2098.

19. Adewuyl YG, Carmlchael GR. Kinetics of oxidation of dimethyl sulfide by hydrogen peroxide in acidic and alkaline medium. Environ. Sci. Technol. 1986; 20:1017–1022. [PubMed: 22257401]

20. Chen KY, Morris JC. Kinetics of oxidation of aqueous sulfide by O_2. Environ. Sci. Technol. 1972; 6:529–537.

21. Hoffmann MR. Kinetics and mechanism of oxidation of hydrogen sulfide by hydrogen peroxide in acidic solution. Environ. Sci. Technol. 1977; 11:61–66.

22. Pikaar I, Rozendal RA, Yuan Z, Keller J, Rabaey K. Electrochemical sulfide oxidation from domestic wastewater using mixed metal-coated titanium electrodes. Water Res. 2011; 45:5381–5388. [PubMed: 21885081]

23. Pikaar I, Rozendal RA, Yuan Z, Keller J, Rabaey K. Electrochemical sulfide removal from synthetic and real domestic wastewater at high current densities. Water Res. 2011; 45:2281–2289. [PubMed: 21300393]

24. Yuan SH, Chen MJ, Mao XH, Alshawabkeh AN. A three-electrode column for Pd-catalytic oxidation of TCE in groundwater with automatic pH-regulation and resistance to reduced sulfur compound foiling. Water Res. 2013; 47:269–278. [PubMed: 23121896]

25. Environmental Protection Administration of China. Water and Wastewater Monitoring and Analysis Methods. 4th. China Environmental Science Press; 2002.

26. Eisenberg G. Colorimetric determination of hydrogen peroxide. Ind. Eng. Chem. Anal. Ed. 1943; 15:327–328.

27. Aikawa B, Burk RC, Sitholé BB. Catalytic hydrodechlorination of 1-chlorooctadecane, 9,10-dichlorostearic acid, and 12,14-dichlorodehydroabietic acid in supercritical carbon dioxide. Appl. Catal. B Environ. 2003; 43:371–378.

28. Chen H, Xu ZY, Wan HQ, Zheng JZ, Yin DQ, Zheng SR. Aqueous bromate reduction by catalytic hydrogenation over Pd/Al_2O_3 catalysts. Appl. Catal. B Environ. 2010; 96:307–313.

29. de Pedro ZM, Casas JA, Gomez-Sainero LM, Rodriguez JJ. Hydrodechlorination of dichloromethane with a Pd/AC catalyst: Reaction pathway and kinetics. Appl. Catal. B Environ. 2010; 98:79–85.

30. Petersen MA, Sale TC, Reardon KF. Electrolytic trichloroethene degradation using mixed metal oxide coated titanium mesh electrodes. Chemosphere. 2007; 67:1573–1581. [PubMed: 17234239]

31. Lowry GV, Reinhard M. Hydrodechlorination of 1- to 3-carbon halogenated organic compounds in water using a palladium catalyst and hydrogen. Environ. Sci. Technol. 1999; 33:1905–1910.

32. Loget G, Zagah D, Bouffier L, Sojic N, Kuhn A. Bipolar electrochemisty: From materials science to motion and beyond. Accounts Chem. Res. 2013 DOI: 10.1021/ar400039k.

33. Munakata N, Reinhard M. Palladium-catalyzed aqueous hydrodechlorination in column reactors: Modeling of deactivation kinetics with sulfite and comparison of regenerants. Appl. Catal. B Environ. 2007; 75:1–10.

34. Chaplin BP, Shapley JR, Werth CJ. The selectivity and sustainability of a Pd-In/gamma-Al_2O_3 catalyst in a packed-bed reactor: The effect of solution composition. Catal. Lett. 2009; 130:56–62.

35. Edwards JK, Solsona B, Ntainjua NE, Carley AF, Herzing AA, Kiely CJ, Hutchings GJ. Switching off hydrogen peroxide hydrogenation in the direct synthesis process. Science. 2009; 323:1037–1041. [PubMed: 19229032]

36. Samanta C. Direct synthesis of hydrogen peroxide from hydrogen and oxygen: An overview of recent developments in the process. Appl. Catal. A. 2008; 350:133–149.

37. Lim TT, Zhu BW. Effects of anions on the kinetics and reactivity of nanoscale Pd/Fe in trichlorobenzene dechlorination. Chemosphere. 2008; 73:1471–1477. [PubMed: 18760820]

38. Schuth C, Disser S, Schuth F, Reinhard M. Tailoring catalysts for hydrodechlorinating chlorinated hydrocarbon contaminants in groundwater. Appl. Catal. B Environ. 2000; 28:147–152.

39. Ranguelova K, Bonini MG, Mason RP. (Bi)sulfite oxidation by copper, zinc-superoxide dismutase: Sulfite-derived radical-initiated protein radical formation. Environ. Health Persp. 2010; 118:970–975.

40. Mottley C, Mason RP, Chignell CF, Sivarajah K, Eling TE. The formation of sulfur trioxide radical anion during the prostaglandin hydroperoxidase-catalyzed oxidation of bisulfite (hydrated sulfur dioxide). J. Biol. Chem. 1982; 257:5050–5055. [PubMed: 6279657]

41. Neta P, Huie RE. Free-radical chemistry of sulfite. Environ. Health Persp. 1985; 64:209–217.

42. Guan YH, Ma J, Li XC, Fang JY, Chen LW. Influence of pH on the formation of sulfate and hydroxyl radicals in the UV/peroxymonosulfate system. Environ. Sci. Technol. 2011; 45:9308–9314. [PubMed: 21999357]

43. Liang SX, Zhao LX, Zhang BT, Lin JM. Experimental studies on the chemiluminescence reaction mechanism of carbonate/bicarbonate and hydrogen peroxide in the presence of cobalt(II). J. Phys. Chem. A. 2008; 112:618–623. [PubMed: 18173250]

44. Bejan D, Guinea E, Bunce NJ. On the nature of the hydroxyl radicals produced at boron doped diamond and Ebonex® anodes. Electrochim. Acta. 2012; 69:275–281.

45. Li R, Kameda T, Toriba A, Hayakawa K, Lin JM. Determination of benzo[α]pyrene-7,10-quinone in airborne particulates by using a chemiluminescence reaction of hydrogen peroxide and hydrosulfite. Anal. Chem. 2012; 84:3215–3221. [PubMed: 22369647]

46. Ranguelova K, Rice AB, Khajo A, Triquigneaux M, Garantziotis S, Magliozzo R, Mason RP. Formation of reactive sulfite-derived free radicals by the activation of human neutrophils: An ESR study. Free Radical Bio. Med. 2012; 52:1264–1271. [PubMed: 22326772]

47. Shi XL, Dalal N, Kasprzak KS. Enhanced generation of hydroxyl radical and sulfur trioxide anion radical from oxidation of sodium sulfite, nickel(II) sulfite, and nickel subsulfide in the presence of nickel(II) complexes. Environ. Health Persp. 1994; 102:91–96.

48. Carter KE, Farrell J. Electrochemical oxidation of trichloroethylene using boron-doped diamond film electrodes. Environ. Sci. Technol. 2009; 43:8350–8354. [PubMed: 19924968]

49. Watts RJ, Washington D, Howsawkeng J, Loge FJ, Teel AL. Comparative toxicity of hydrogen peroxide, hydroxyl radicals, and superoxide anion to Escherichia coli. Adv. Environ. Res. 2003; 7:961–968.

50. Martínez-Huitle CA, Brillas E. Electrochemical alternatives for drinking water disinfection. Angew. Chem. Int. Ed. 2008; 47:1998–2005.
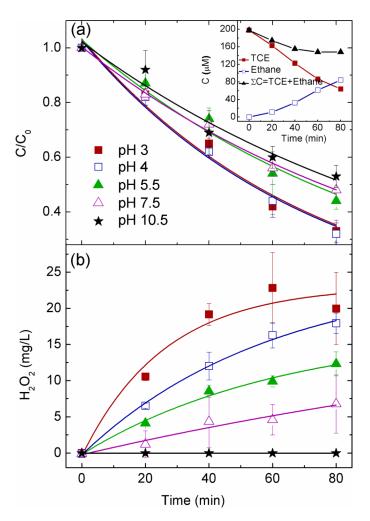
Figure 1.
(a) TCE hydrodechlorination and (b) H_2O_2 production at different pH. Inset graph in (a) is the transformation profile of TCE at pH 4. The transformation conditions are based on 198 μM initial TCE concentration, 1 g/L Pd/Al_2O_3 and 10 mM Na_2SO_4 background electrolyte. The pH refers to the initial solution pH. Curves in (a) refer to the fittings by pseudo-first-order kinetic model.
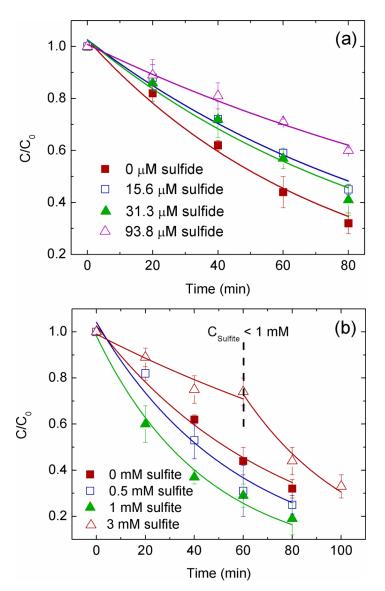
Figure 2.
Effect of (a) sulfide and (b) sulfite on TCE hydrodechlorination. The transformation conditions are based on 198 μM initial TCE concentration, pH 4, 1 g/L Pd/Al$_2$O$_3$ and 10 mM Na$_2$SO$_4$ background electrolyte. Curves refer to fittings by pseudo-first-order kinetic model.
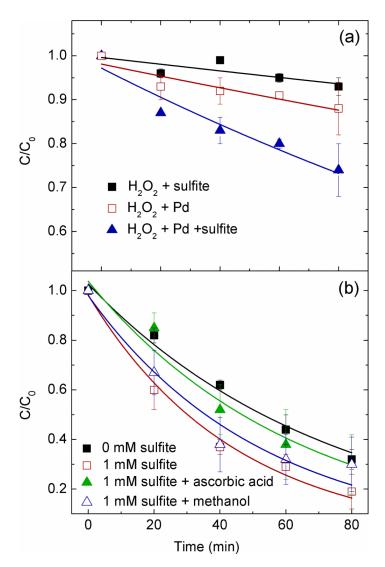
Figure 3.
(a) Effect of sulfite on TCE transformation by H_2O_2 without electricity, (b) effect of radical scavengers on TCE transformation, Unless otherwised specified, the transformation conditions for (a) are based on 100 mg/L H_2O_2, 1 mM sulfite, 1 g/L Pd/Al_2O_3, pH 4 and 10 mM Na_2SO_4, and for (b) based on 198 μM initial TCE concentration, pH 4, 1 g/L Pd/Al_2O_3 and 10 mM Na_2SO_4. The concentrations of methanol and ascorbic acid in (b) are 60 and 10 mM, respectively. Error bars in (b) are not given in order to give clear comparison. Curves refer to fittings by pseudo-first-order kinetic model.
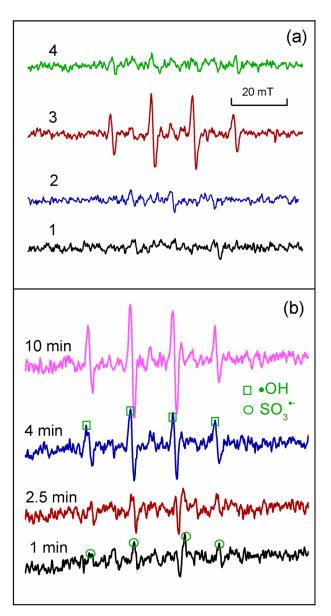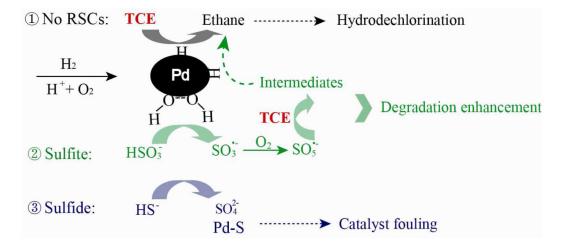
Figure 4.
(a) ESR spectra of radicals generated in the system, Curve 1: electrolysis without Pd/Al_2O_3 but with 1 mM sulfite; Curve 2: electrolysis with 1 g/L Pd/Al_2O_3 but without sulfite; Curve 3: electrolysis with 1 g/L Pd/Al_2O_3 and 1 mM sulfite; Curve 4: electrolysis with 1 g/L Pd/Al_2O_3 and 3 mM sulfite. The measurement is performed within 10 min. (b) Evolution of ESR signals with the mixing time for sample specified in Curve 3 in (a). Unless otherwised specified, the reaction conditions are based on pH 4, 100 mA, and 10 mM Na_2SO_4.

Scheme 1.
Proposed mechanism for the distinct influence of sulfide and sulfite on TCE hydrodechlorination under oxidizing conditions

Table 1

Results Summarized for TCE Hydrodechlorination and H_2O_2 Accumulation in the Batch Experiments

no.	Variation parameters[a]	Final pH	Removal (%)[b]	H_2O_2 (mg/L)[c]	k_{obs} (min^{-1})[d]	R^2
1	pH 3.00	2.93 ± 0.01	67.2 ± 3.9	20.0 ± 5.0	0.013 ± 0.001	0.969
2	pH 4.00	3.49 ± 0.01	67.6 ± 3.6	19.2 ± 1.5	0.014 ± 0.001	0.984
3	pH 5.50	3.94 ± 0.03	55.7 ± 3.3	13.2 ± 1.8	0.010 ± 0.001	0.967
4	pH 7.50	4.64 ± 0.17	51.8 ± 0.4	7.3 ± 4.3	0.009 ± 0.000	0.992
5	pH 10.50	10.41 ± 0.28	46.9 ± 4.4	0 ± 0	0.009 ± 0.001	0.955
6[e]	Cathodic compartment	> 10	100 ± 0	0 ± 0	0.071 ± 0.012	0.912
7	0 mM sulfite	3.49 ± 0.01	67.6 ± 3.6	19.2 ± 1.5	0.014 ± 0.001	0.984
8	0.5 mM sulfite	3.22 ± 0.04	74.9 ± 4.4	19.4 ± 2.8	0.017 ± 0.002	0.961
9	1 mM sulfite	3.15 ± 0.06	81.3 ± 6.7	13.2 ± 0.4	0.022 ± 0.002	0.988
10[f]	3 mM sulfite	2.84 ± 0.05	66.9 ± 5.4	8.2 ± 0.2	0.006 ± 0.001	0.906
					0.022 ± 0.003	0.961
11	0 μM sulfide	3.49 ± 0.01	67.6 ± 3.6	19.2 ± 1.5	0.014 ± 0.001	0.984
12	15.6 μM sulfide	3.65 ± 0.03	55.5 ± 2.3	20.8 ± 0.8	0.009 ± 0.001	0.979
13	31.3 μM sulfide	3.56 ± 0.07	58.9 ± 5.9	21.7 ± 1.0	0.010 ± 0.001	0.971
14	93.8 μM sulfide	3.71 ± 0.07	39.9 ± 0.9	13.8 ± 0.2	0.006 ± 0.000	0.987

[a]Otherwise stated, the reaction conditions are based on 198 μM TCE, pH 4, 1 g/L Pd/Al$_2$O$_3$, 100 mA, 10 mM Na$_2$SO$_4$ and 80 min reaction.

[b]Removal is the percentage of TCE reduction at 80 min.

[c]The H_2O_2 concentrations refer to the final accumulated concentrations.

[d]k_1 is the observed pseudo-first-order kinetic constant, respectively.

[e]In the cathodic compartment, the reaction conditions are based on 198 μM initial TCE concentration, intial solution pH 4, 50 mA, 1 g/L Pd/Al$_2$O$_3$ and 10 mM Na$_2$SO$_4$ background electrolyte. O$_2$ was purged by bubbling pure N$_2$ before electrolysis. The cathodic compartment is separated with anodic compartment by a Nafion membrane and has the same diameter as the undivided cell.

[f]For the influence of 3 mM sulfite, the process lasts for 100 min, and the reaction in first 60 min and after 60 min are separately fitted by pseudo-first-order kinetics.